

Dual Role of VAMP8 in Regulating Insulin Exocytosis and Islet β Cell Growth

Dan Zhu,^{1,2,8} Yi Zhang,^{1,2,8} Patrick P.L. Lam,^{1,2,8} Subhankar Dolai,^{1,2,8} Yunfeng Liu,^{1,2,8} Erica P. Cai,³ Diana Choi,³ Stephanie A. Schroer,³ Youhou Kang,^{1,2} Emma M. Allister,^{1,2} Tairan Qin,^{1,2} Michael B. Wheeler,^{1,2} Cheng-Chun Wang,⁴ Wan-Jin Hong,^{4,5} Minna Woo,^{3,6,7} and Herbert Y. Gaisano^{1,2,3,*}

¹Department of Medicine

²Department of Physiology

³Institute of Medical Science

University of Toronto, Toronto, ON M5S 1A8, Canada

⁴Institute of Molecular and Cell Biology, Proteos, Singapore 138673, Republic of Singapore

⁵School of Pharmaceutical Sciences, Xiamen University, Xiamen 361005, China

⁶Toronto General Research Institute, Toronto, ON M4G 2C4, Canada

⁷Department of Medicine and Keenan Research Centre at Li Ka Shing Knowledge Institute, St. Michael's Hospital, Toronto, ON M5G 2M9, Canada

⁸These authors contributed equally to this work

*Correspondence: herbert.gaisano@utoronto.ca

<http://dx.doi.org/10.1016/j.cmet.2012.07.001>

SUMMARY

Optimal insulin secretion required to maintain glucose homeostasis is the summation of total pancreatic islet β cell mass and intrinsic secretory capacity of individual β cells, which are regulated by distinct mechanisms that could be amplified by glucagon-like-peptide-1 (GLP-1). Because of these actions of GLP-1 on islet β cells, GLP-1 has been deployed to treat diabetes. We employed SNARE protein VAMP8-null mice to demonstrate that VAMP8 mediates insulin granule recruitment to the plasma membrane, which partly accounts for GLP-1 potentiation of glucose-stimulated insulin secretion. VAMP8-null mice also exhibited increased islet β cell mass from increased β cell mitosis, with β cell proliferative activity greatly amplified by GLP-1. Thus, despite the β cell exocytotic defect, VAMP8-null mice have an increased total insulin secretory capacity, which improved glucose homeostasis. We conclude that these VAMP8-mediated events partly underlie the therapeutic actions of GLP-1 on insulin secretion and β cell growth.

INTRODUCTION

Diabetes is a disease in which pancreatic islet β cells' insulin secretory capacity eventually fails to meet glycemic demand, resulting in poor glucose homeostasis that leads to acute and chronic complications (Kahn, 1998). Great efforts have thus been directed at elucidating underlying disease mechanisms toward clever strategies to rescue the defective glucose-stimulated insulin secretion (GSIS) and/or increase β cell growth. Glucagon-like peptides, particularly GLP-1, have become a panacea in achieving both lofty therapeutic goals in the treatment of diabetes (Lovshin and Drucker, 2009). Nonetheless,

the precise mechanisms by which GLP-1 influences GSIS and β cell growth remain unclear.

Efficacious insulin secretion requires effective coupling of agonist- (glucose, GLP-1) evoked signaling pathways to insulin secretory granule (SG) exocytosis machineries. A mode of insulin exocytosis is fusion of docked insulin SGs with the plasma membrane (PM), mediated by a multimolecular complex of fusion molecules, including SNARE (v- and t-SNAREs) and the associated protein components (nSec/Munc18 or SM proteins, Munc13) (Kwan and Gaisano, 2009; Südhof and Rothman, 2009). Alternate modes of exocytosis include newcomer SGs that undergo little or no docking time at the PM before fusion, which occurs at high frequency, and SG-SG fusion after SG-PM fusion, termed sequential exocytosis, which occurs at low frequency in β cells (only 2%) (reviewed in Gaisano, 2012). Both of these latter exocytotic events become substantially up-regulated by GLP-1 to account for large portions of GLP-1-potentiated GSIS (Kwan and Gaisano, 2005). The SM/SNARE complex, which includes Syntaxin-1A (Syn-1A) and Munc18a, mediates fusion of predocked insulin SGs, accounting for the first phase of GSIS (Ohara-Imaizumi et al., 2007). The other exocytotic proteins that mediate newcomer SGs and SG-SG fusions remain to be defined.

VAMP8 was first identified as an endosomal SNARE (endobrevin) involved in endosomal fusion (Antonin et al., 2000a, 2000b; Wong et al., 1998). It was then implicated in GLUT4 exocytosis (Zhao et al., 2009) and endocytosis (Williams and Pessin, 2008). However, VAMP8 played a nonessential role in these membrane fusion processes because of functional redundancy provided by other VAMPs (Antonin et al., 2000a, 2000b; Zhao et al., 2009). In regulated exocytosis, VAMP8 has been implicated in several secretory cells, including pancreatic acini (Wang et al., 2004) and other exocrine tissues (Wang et al., 2007), platelets (Ren et al., 2007), basophils (Lippert et al., 2007), mast cells (Tiwari et al., 2008), lymphocytes (Loo et al., 2009), and kidney collecting duct cells (Wang et al., 2010). For exocytosis, VAMP8 interacts robustly with SNAP23 and Syn-4 (Wang et al., 2004, 2007, 2010) and the SM protein Munc18c (Cosen-Binker

et al., 2008). For endocytosis, cognate t-SNAREs are Vti1a or Vti1b (Antonin et al., 2000a). In exocrine pancreas, VAMP8 mediates not only SG-PM exocytosis, but also SG-SG fusion, the latter involving a distinct SM/SNARE complex that includes Munc18b, SNAP23, and Syn-3 (Cosen-Binker et al., 2008).

In the current work, we employed VAMP8-null mice (Cosen-Binker et al., 2008; Wang et al., 2004) to show that GLP-1-potentiated islet GSIS was reduced because of deficient recruitment of newcomer SGs to the PM and could be rescued to fully restore biphasic GSIS by VAMP8 re-expression. Surprisingly, VAMP8-null mice paradoxically exhibited increased β cell proliferation and mitosis, which could be upregulated by GLP-1 to amplify β cell mitosis. Thus, in islet β cells, VAMP8 plays dual and nonredundant roles in insulin exocytosis and β cell proliferation, which could potentially impact diabetes therapy.

RESULTS

VAMP8 Mediates GLP-1-Potentiated GSIS

VAMP8 knockout (KO) mice were backcrossed to 129SvJ for seven generations to reduce contamination from its original mixture with C57/BL6 background. In pancreatic islets of WT mice (litter controls), VAMP8 was found to be in β cells but not in α cells (Figure S1A available online), where a majority (>90%) of VAMP8 was colocalized with insulin SGs (Figure 1A, top panels). A minority of VAMP8 was colocalized with early endosomes (EEA1, Figure 1A, middle panels) and lysosomes (LAMP1, Figure 1A, bottom panels) as previously reported (Antonin et al., 2000b; Wong et al., 1998). Western blotting of islets from litter control WT and VAMP8 KO mice confirmed the absence of VAMP8, whereas levels of cognate and noncognate syntaxins, SNAP25, and SM proteins were not altered by VAMP8 deletion (Figure 1B). We examined the physiologic biphasic GSIS by employing an islet perfusion assay. There was no difference in 16.7 mM GSIS in first- (PH1, first 20 min) or second- (PH2, next 20 min) phase secretion (Figure 1C). However, when islets were pretreated with GLP-1 (10 nM, plus 150 μ M IBMX) to induce cAMP-potentiated secretion, secretory responses were reduced by 46% at PH1 and 32% at PH2 in VAMP8 KO islets (PH1, 79 ± 19 ; PH2, 141 ± 13) compared to WT islets (PH1, 146 ± 4 ; PH2, 207 ± 13 , Figure 1D). To confirm that this reduced secretory response was attributed to VAMP8 deficiency per se, we transduced VAMP8 KO islets with adenoviruses expressing VAMP8 (Ad-VAMP8-GFP, 70% transfection efficiency by GFP fluorescence), which fully restored PH1 (192 ± 20) and PH2 (279 ± 43) (Figure 1E) secretion compared to Ad-GFP expression (PH1, 102 ± 6 ; PH2, 135 ± 24); this was an increase of 88% and 107%, respectively.

Insulin content per islet from VAMP8 KO mice was higher than WT mice islets (Figure S1B), raising the possibility of a higher β cell number in VAMP8 KO islets. However, in islet perfusion assays, insulin released was always normalized to total islet insulin content to negate such bias. Nonetheless, we assessed the exocytotic capacity of single β cells by employing patch-clamp membrane capacitance measurements (Cm) using a serial depolarization protocol (Figure 1F), wherein the first two pulses estimate the readily releasable pool (RRP) and succeeding pulses (third to tenth) measure RRP refilling, postulated to corre-

spond to PH1 and PH2 of GSIS, respectively (Rorsman and Renström, 2003). In absence of cAMP in the patch pipette (Figure 1F), Δ Cm in WT and VAMP8 KO β cells were comparable. In presence of cAMP (0.1 mM) and glucose (16.7 mM) (Figure 1G) to simulate GLP-1-potentiated GSIS as in the islet perfusion study (Figure 1D), RRP (6.5 ± 0.6) and RRP refilling (18.5 ± 1.2) were reduced in VAMP8 KO β cells by 34% and 23%, respectively, compared to WT β cells (RRP, 9.8 ± 1.2 ; RRP refilling, 24.0 ± 2.1). To ensure that the effects of VAMP8 or its absence are on exocytosis per se, and not due to effects on Ca^{2+} influx during PM depolarization, we showed integrated Ca^{2+} currents during depolarization to be similar between the two groups (Figure 1H).

VAMP8 Recruits Newcomer Granules to Plasma Membrane to Undergo Exocytosis

We examined how changes in single SG fusion dynamics would account for the above secretory results by employing time-lapse total internal reflection fluorescence microscopy (TIRFM) to monitor exocytosis dynamics of insulin SGs tagged with neuropeptide Y (NPY)-EGFP by adenovirus transduction (Ad-NPY-EGFP) of mice β cells. At the basal unstimulated state (Figure 2A), punctate fluorescence indicating docked SGs was not different between WT ($10.2 \pm 0.624 / 100 \mu\text{m}^2$) and KO ($10.4 \pm 0.817 / 100 \mu\text{m}^2$) β cells. When cells were stimulated with 16.7 mM glucose plus 10 nM GLP-1, the SG densities of WT β cells examined per image serially were observed to be increasing compared to a slight decrease from basal levels in KO β cells (Figure S2A), which is largely contributed by a more sustained increase in newcomer SGs toward the PM in WT β cells. Consistently, assessment of cumulative fusion events over time (Figure 2B) showed much less fusion events during the 18 min stimulation in KO β cells than in WT β cells.

We then dissected the single SG fusion dynamics (Figure 2C). At 2.8 mM glucose, either in the absence or presence of GLP-1, we seldom found spontaneous fusion events (Figure 2D). When 16.7 mM glucose was added (after preincubation with GLP-1 plus IBMX), single SG fusion events were observed as flashes of fluorescence that rapidly dissipate in a cloud-like diffusion pattern. However, these exocytotic events were not uniform from the same group of SGs, but could be categorized into three distinct modes (Figure 2C). “Predock” fusion mode (Figure 2C, top; Figure 2D, blue) refers to SGs that were already docked onto the PM (as Figure 2A) for a period of time prior to stimulation. Newcomer SGs refer to new SGs appearing de novo after stimulation within the evanescent field that then undergo exocytosis, which can be categorized into two distinct patterns (Kasai et al., 2008; Shibasaki et al., 2007) designated as “no-dock” (Figure 2C, middle) and “short-dock” (Figure 2C, bottom) newcomers. No-dock newcomer SGs (Figure 2D, red) are newly recruited by stimulation and immediately fused with the PM (a docking state <200 ms, minimal interval between two consecutive frames). Short-dock newcomer SGs (Figure 2D, green) are those newly recruited by stimulation that first docked for some residence time at the PM varying from seconds to minutes and then fused with the PM. Even in PH1 GSIS, newcomer SGs already accounted for >70% of exocytotic events in WT β cells (Figure 2D, top), which corresponded to the diverging cumulative increase in exocytosis in WT β cells compared to KO cells

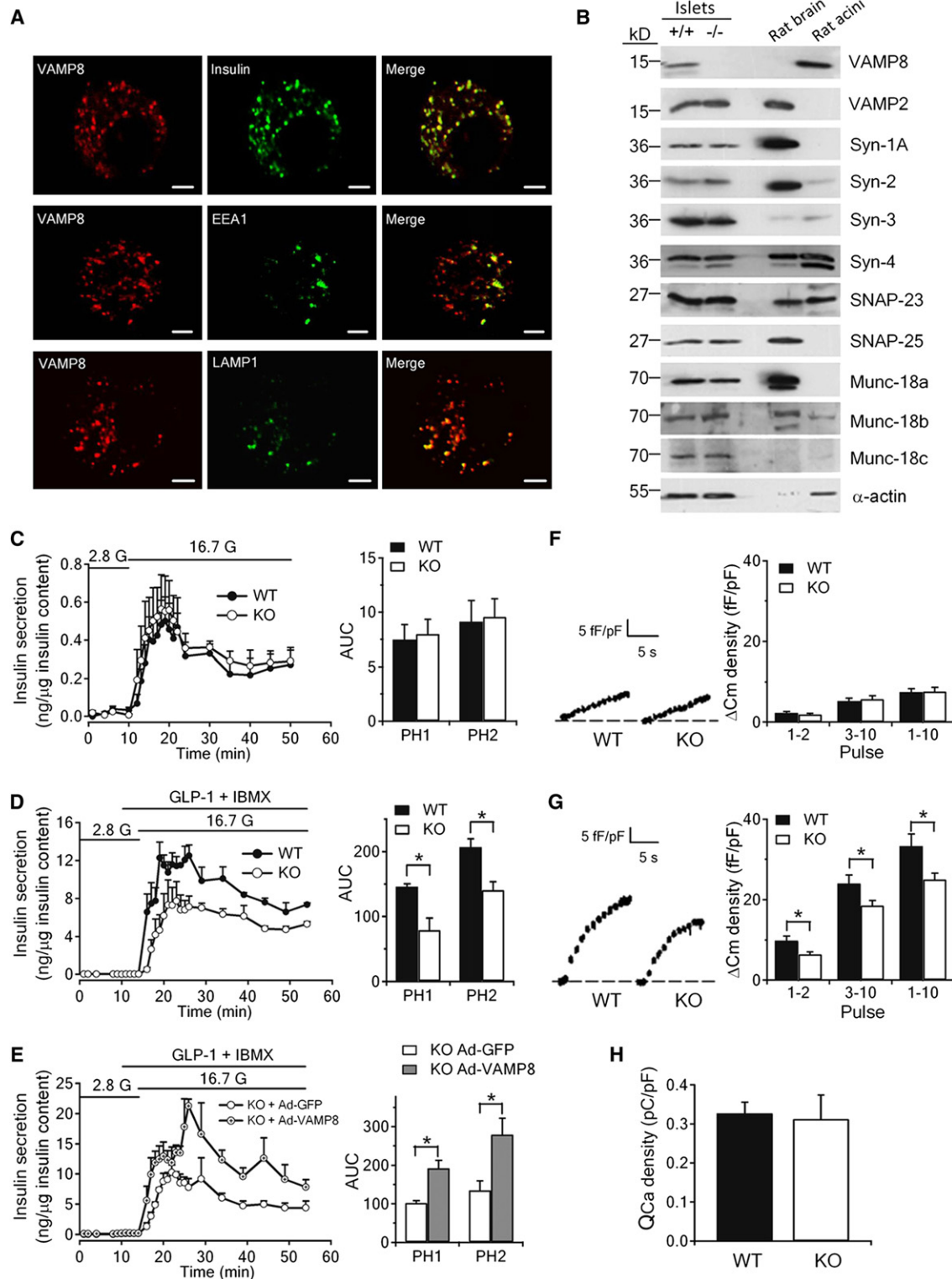


Figure 1. VAMP8 Deletion Abolishes GLP-1-Potentiated GSIS in Pancreatic β Cells

(A) Representative immunofluorescence images of VAMP8 (red) with insulin (green), early endosomes (EEA1 antibody, green), or lysosomes (LAMP1 antibody, green) in mouse pancreatic β cells, with their colocalization shown in merge images (yellow). Shown are representative images of three independent experiments. Scale bars represent 3 μ m.

(B) Western blotting analysis of SNARE and SNARE-associated protein expression in pancreatic islets of WT and VAMP8 KO mice. Pancreatic acini and brain used as positive and negative controls.

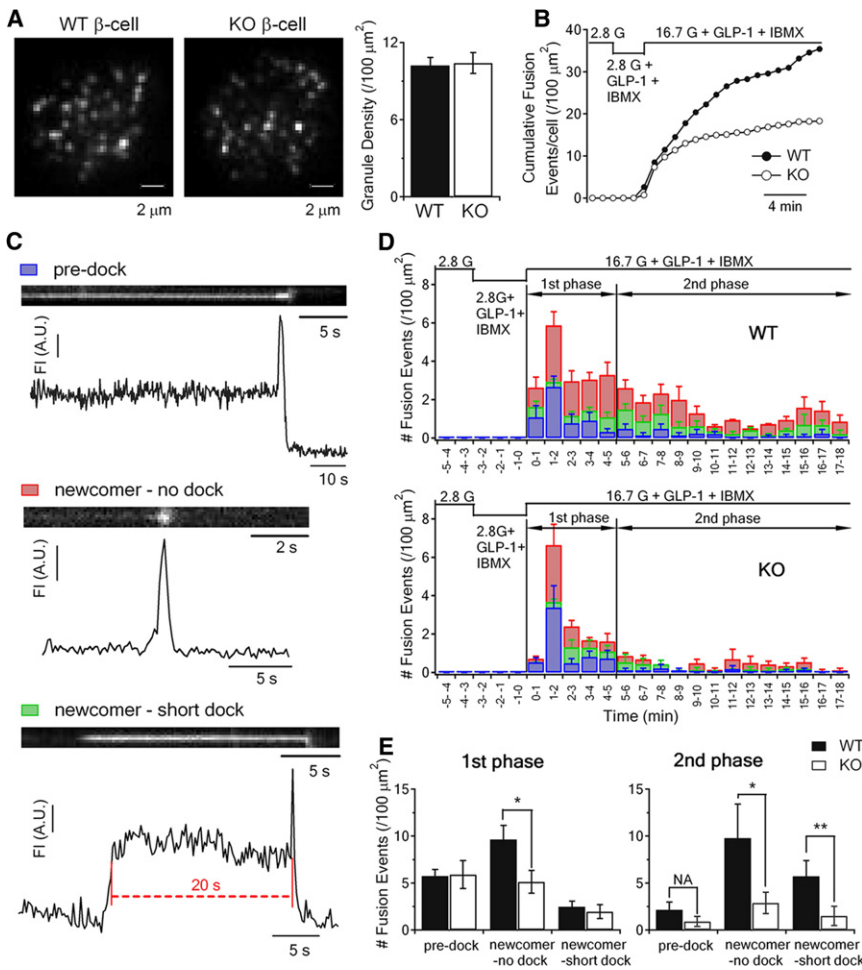


Figure 2. VAMP8 Mediates Exocytosis of Newcomer Insulin Granules

(A) Left: TIRF images of docked insulin SGs in WT or *VAMP8* KO islet β cells. Scale bars represent 2 μ m. Right: Comparison of averaged SG densities before stimulation. Summary graph is shown as means \pm SEMs, not significant. (B) Normalized cumulative fusion events of insulin SGs per cell per 100 μ m² stimulated as indicated. (C) Kymographs and corresponding fluorescence intensity curves showing three modes of insulin SG fusion events in islet β cells: “pre-dock” (blue bar), “newcomer - no dock” (red bar), and “newcomer - short dock” (green bar) (shown is 20 s docking time before undergoing fusion). Data are shown as means \pm SEMs. (D) Histogram of different fusion events in the the first phase (first 5 min after 16.7 mM glucose stimulation) and second phase (5–18 min) in WT versus KO β cells. Data obtained from five independent experiments (three to five cells from each experiment; WT = 16 cells, KO = 18 cells), expressed as mean \pm SEMs. (E) Summary of the three modes of fusion events in the first (left) and second phases (right), shown as means \pm SEMs. **p* < 0.05, ***p* < 0.01. See also Figure S2.

(Figure 2B). However, fusion events of predock SGs (summary analysis, Figure 2E) were similar between WT and KO β cells in PH1 and PH2 GSIS. To confirm, we assessed exocytosis evoked by 50 mM K⁺ stimulation, which causes fusion of predocked SGs predominantly (~68% of total fusion). There was no difference between KO and WT β cells in fusion events of predocked SGs occurring in the first 5 min (Figures S2B–S2D). Thus, reduction of exocytosis in both phases of secretion evoked by 16.7 mM glucose and GLP-1 was accounted for entirely from reduction in newcomer SGs. In PH1 GSIS, there was reduction in only no-dock newcomer SGs (WT 9.62 \pm 1.52 versus KO 5.72 \pm 0.71/100 μ m²); reduction in PH2 GSIS included both no-dock (red bars; WT, 9.78 \pm 3.62 versus KO, 2.88 \pm 1.13/100 μ m²)

and short-dock (green bars; WT 5.71 \pm 1.69 versus KO 1.51 \pm 1.02/100 μ m²) newcomer SGs (summary analysis, Figure 2E). These results taken together indicate that VAMP8 mediated the recruitment and exocytotic fusion of newcomer SGs, but not of previously docked SGs. We probed for SM/SNARE complexes that might mediate these distinct exocytotic events, including newcomer SGs and predock SG fusion. We immunoprecipitated (IPed) three major exocytotic Syntaxins (Syn-1, Sn-2, and Syn-3) from INS-1 cells at basal (0.8 mM glucose, Figures 3A and 3B), high-glucose (16.7 mM glucose only, Figure 3B), and maximal (GLP-1 potentiated) stimulated conditions (16.7 mM glucose plus 10 nM GLP-1 with IBMX, Figures 3A and 3B) and examined which cognate SNAREs and SM protein partners were co-IPed. The INS-1 cell line was used to provide more abundant protein than islets required for IP assays. As predicted, under basal conditions, Syn-1A, known to mediate fusion of docked SGs, co-IPed Munc18a but minimal SNAP25 and VAMP2; in high-glucose stimulation and more so under GLP-1/IBMX potentiation, Syn-1A also co-IPed abundant

(C–E) Islet perfusion assays in WT and *VAMP8* KO mice pancreatic islets (left), and corresponding AUCs (area under the curve) of insulin release (right) during islet perfusion, stimulated by 16.7 mM glucose only (C), GLP-1 (10 nM) plus IBMX (150 μ M) with 16.7 mM glucose (D), or GLP-1 plus IBMX with glucose in *VAMP8* KO islets infected with Ad-VAMP8 or Ad-GFP (E). *n* = 4–5 per group. Summary graphs shown as means \pm SEMs. **p* < 0.05. (F and G) Changes in cell C_m (Δ C_m) in response to trains of 500 ms depolarization pulses in WT and *VAMP8* KO β cells. Left: Representative recordings of Δ C_m normalized to basal cell C_m (in fF/pF) evoked by depolarizations alone (F) (KO, *n* = 32; WT, *n* = 35) or with 16.7 mM glucose and 0.1 mM cAMP (G) (KO, *n* = 64; WT, *n* = 70). Right: Summary of C_m evoked by the first two pulses (pulses 1–2), last eight pulses (pulses 3–10), and all ten pulses (pulses 1–10). Summary graphs shown as means \pm SEMs. **p* < 0.05. (H) Summary of integrated Ca²⁺ currents (QCa) evoked by depolarization pulses from –70 to 0 mV (*n* = 11–12 per group). Summary graph is shown as means \pm SEMs, not significant. See also Figure S1.

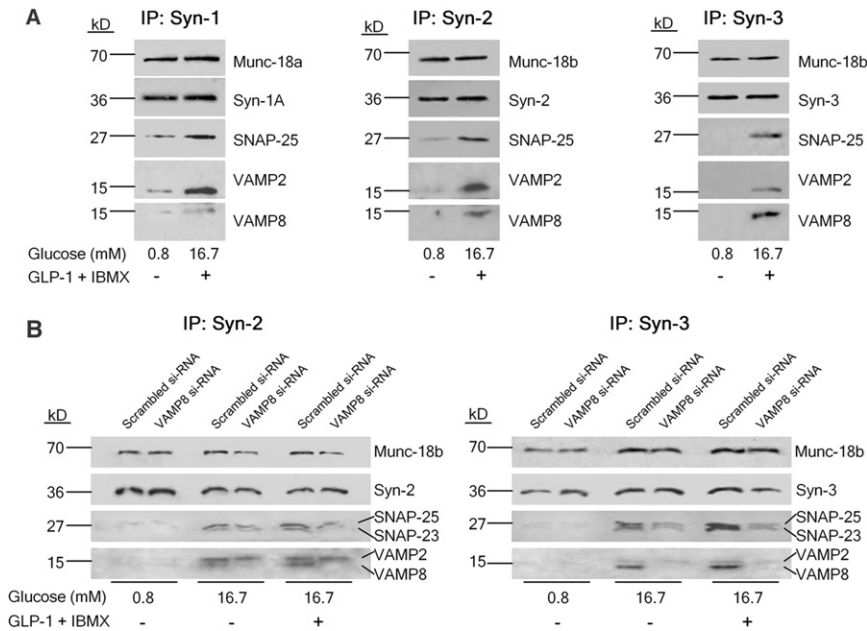


Figure 3. VAMP8 Preferably Binds to Syn-2 or Syn-3 but Not Syn-1 in Forming SNARE Complexes

(A) Co-IP assays showing Syntaxin 1A, 2 and 3 formed SM/trans-SNARE complexes in INS-1 cells after stimulation.

(B) Western blots shows co-IP of Syn-2 (left) or Syn-3 (right) with indicated SNARE/SM proteins in control or VAMP8 siRNA-transduced INS-1 cells, treated as indicated. Scrambled nonsense siRNA was transduced as controls. Syn-1A co-IP was also performed, as shown in Figure S3C.

Studies in (A) and (B) are each representative of three independent experiments with samples performed in duplicate; statistical analysis is in Figure S3D. Input controls in Figure S3B showed no changes in levels of total lysate proteins. See also Figure S3.

VAMP8 Deletion Paradoxically Increases β Cell Mass

Reduction of individual β cell insulin exocytosis by VAMP8 deletion (Figures

3A, S3C, and S3D). Syn-2 and Syn-3 co-IPed abundant Munc18b at basal condition; in high-glucose stimulation and more so under GLP-1/IBMX potentiation, Syn-2 and Syn-3 also co-IPed abundant SNAP25, SNAP23, and VAMP8 (Figures 3A and 3B). While Syn-2 and Syn-3 also co-IPed VAMP2, Syn-2 preferred VAMP2, and Syn-3 preferred VAMP8. Amounts of SM/SNARE complexes precipitated were notably more after GLP-1-potentiated GSIS than after high-glucose stimulation (Figure S3D). These SM-SNARE complexes formed by Syn-2 and Syn-3 are reminiscent of our recent report in pancreatic acini, in which similar SNARE/SM complexes were co-IPed (Cosen-Binker et al., 2008). In that report, we postulated that Syn-2/VAMP2/SNAP23/Munc8b mediated SG exocytosis with apical PM and that Syn-3/VAMP8/SNAP23/Munc18b mediated SG-SG fusion.

We next investigated whether formation of SM/SNARE complexes could be altered by depletion of VAMP8. Expression of endogenous levels of VAMP8 in INS-1 was reduced by 88.2% by small interfering RNA (siRNA) treatment (compared to scrambled siRNA), which caused reduced amounts of SNAP25 and SNAP23 to be co-IPed by Syn-2 and Syn-3, with no influence on VAMP2 (Figure 3B). This suggests that VAMP8 depletion negatively affected the stability of Munc18b/Syn-3 and Syn-2 complex with SNAP25 and SNAP23. VAMP8 may thus mediate newcomer SG fusion with the PM by its interactions with Syn-3 or Syn-2. While not assessed in our TIRFM study, a small amount of SG-SG fusion occurs in β cells, better assessed by two-photon microscopy (Takahashi et al., 2002, 2004) and reported to be also amplified by GLP-1 potentiation (Kwan and Gaisano, 2005), and it may be mediated by one of these SM/SNARE complexes as postulated for pancreatic acini (Cosen-Binker et al., 2008). SNAP23 might play a redundant role to SNAP25 (Sadoul et al., 1997), but its precise role in insulin exocytosis has not been determined. Syn-1A SM-SNARE complexes (Figure S3C) were not at all altered by VAMP8 depletion, thus enabling fusion of predocked SGs (Figures S2B–S2D).

1 and 2) would be expected to reduce overall in vivo insulin secretory capacity, which would result in abnormal glucose homeostasis. We thus proceeded to conduct an intraperitoneal (i.p.) glucose tolerance test (IPGTT) to confirm this. Very surprisingly, VAMP8 KO mice exhibited a paradoxical response of better glucose tolerance than WT mice (Figure 4A). In fact, plasma insulin collected during IPGTT showed correspondingly higher insulin levels in KO mice versus WT mice (Figure 4B, corresponding area under the curve [AUC] shown on the right). During the preparation of this work, a report employing VAMP8 KO mice on a mixed but predominant C57/BL6 insulin resistance-prone background showed that VAMP8 deletion increased sarcolemmal GLUT4 levels, thus improving insulin sensitivity (Zong et al., 2011). We thus performed insulin tolerance tests and found that our VAMP8 KO mice on a dominant 129SvJ background exhibit comparable insulin sensitivity in peripheral tissues between VAMP8 KO and WT mice (Figure 4C), suggesting that differences in insulin sensitivity between the two studies were in part accounted for by differences in genetic background.

Since VAMP8 influenced β cell secretion, it's possible that global VAMP8 deletion could also alter intestinal L cell secretion of incretin hormones, GLP-1, and gastric inhibitory polypeptide (GIP), which could in turn potentiate GSIS (and β cell growth—see below). We thus examined GLP-1 and GIP secretion in response to oral GTT (OGTT). Basal and peak plasma levels of total GLP-1 and GIP were similar between WT and KO mice (Figure 4D); the better glucose tolerance and higher insulin levels in KO mice were confirmed (Figures S4A and S4B).

Thus, the next plausible explanation for the apparent discrepancy between reduced exocytosis of individual VAMP8 KO β cells and higher in vivo insulin secretion would be that VAMP8 KO mice might have increased β cell mass whereby a much large number of β cells could collectively secrete more insulin in vivo. We examined the islet mass in infant (2-week-old) and adult (6- to 12-week-old) mice. Islets of 2-week-old

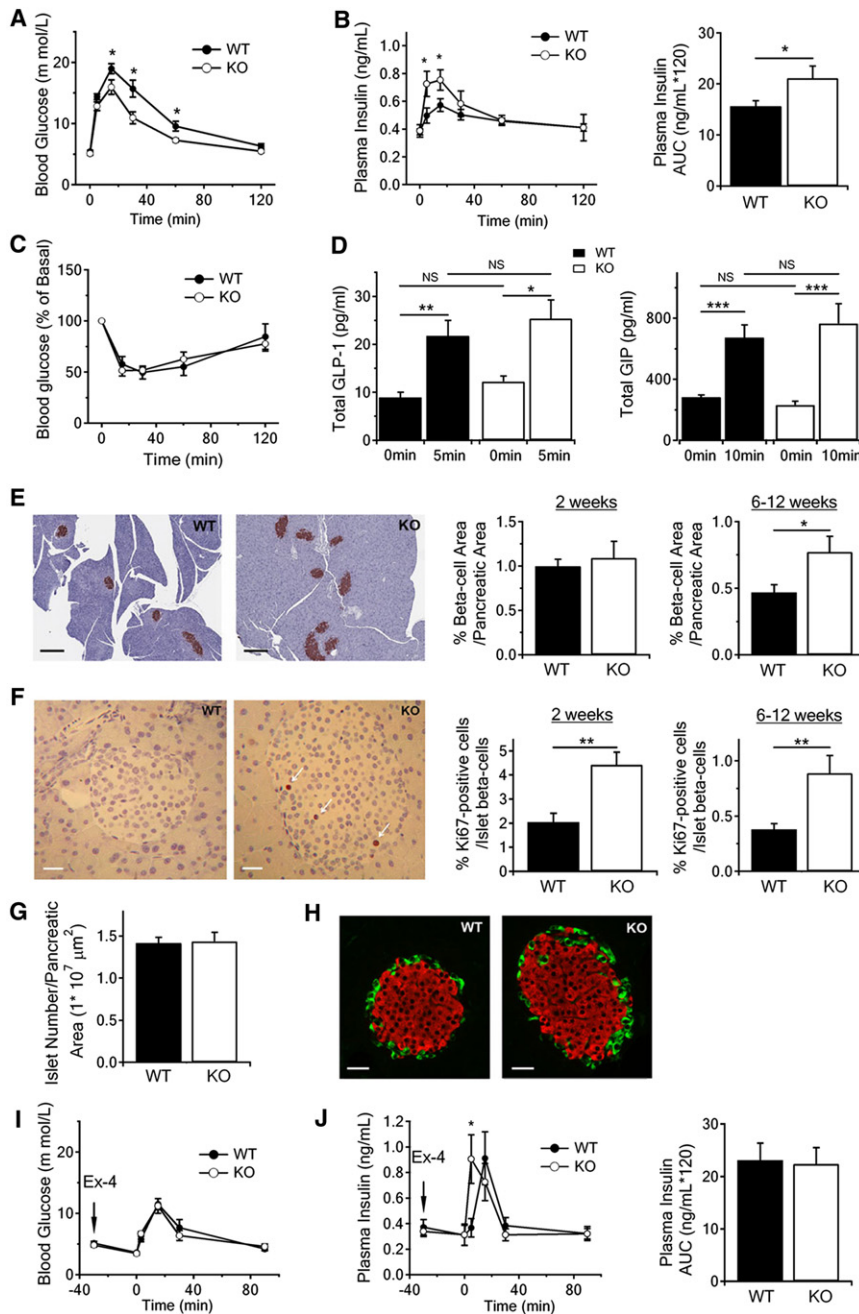


Figure 4. VAMP8 Deletion Caused an Increase in Islet β Cell Mass, which Improved Glucose Homeostasis

(A, B, I, and J) IPGTTs were performed without (A and B) or with (I and J) 30 min Ex-4 pretreatment, with blood glucose levels (A and I) and insulin secretion (B and J) assessed during IPGTT. Insulin secretion is also shown as AUC encompassing 120 min of IPGTT (right panels). n = 10 for each group.

(C) Blood glucose levels during IPITT. n = 8 for each group.

(D) OGTTs performed on age-matched male mice and circulating levels of total GLP-1 (left) and GIP immunoreactivity (right) were measured before and after oral glucose administration. Corresponding levels of blood glucose and insulin are shown in Figures S4A and S4B, respectively. n = 10 for each group. Summary graphs shown as means \pm SEMs.

(E–H) VAMP8 deletion leads to increased β cell area and proliferation.

(E) Insulin-immunostained pancreatic sections (left). Scale bars represent 200 μm ; β cell area per pancreatic area ratios on 2-week-old (middle) or 6- to 12-week-old (right) mouse pancreatic sections.

(F) Islet architecture shown in Ki67-stained pancreatic sections (white arrows indicate Ki67-positive signals) (left). Scale bars represent 20 μm ; Ki67-positive islet β cells as percentage of total islet β cells on 2-week-old (middle) or 6- to 12-week-old (right) mouse pancreatic sections are shown.

(G) Islet numbers per total pancreas area.

(H) Islet architecture shown as insulin (red) and glucagon (green) staining on pancreatic sections. Scale bars represent 40 μm .

Results are shown as means \pm SEMs, n = 10–11 mice for each. *p < 0.05; **p < 0.01; ***p < 0.001. See also Figure S4.

mice did not show larger β cell mass (Figure 4E, middle) but already displayed increased β cell proliferative activity indicated by a larger number of Ki67-positive β cells (Figure 4F, middle, and Figure S4C). In contrast, 6- to 12-week-old VAMP8 KO islets at basal condition showed an increase in β cell area per pancreatic area (Figure 4E, left and right) along with increased percentage of Ki67-positive β cells in KO mice versus WT mice (Figure 4F, left and right, and Figure S4D). There were no changes in the number of islets (Figure 4G). Taken together, these results suggest that VAMP8 regulates β cell proliferation shortly after birth rather than the formation of new β cells that would have otherwise increased islet

not play a role in organization of different islet cell subsets (Figure 4H).

We then examined whether the increased mass of β cells in VAMP8 KO mice would be responsive to clinically used long-acting GLP-1 analog exendin-4 (Ex-4) in potentiating GSIS in vivo. VAMP8 KO mice pretreated with Ex-4 followed by i.p. glucose stimulation exhibited only a similar potentiated increase in plasma insulin release (although earlier peak) as WT mice (Figure 4J), thus attaining similar blood glucose levels (Figure 4I). These results indicate that the smaller islet β cell mass in WT mice has similar maximal insulin secretory capacity as the larger KO β cell mass, suggesting that maximal insulin secretory

capacity of individual β cells from *VAMP8* KO mice islets would have to be reduced, consistent with the *in vitro* results in Figures 1 and 2. These results suggest that GLP-1-potentiated GSIS is primarily mediated by VAMP8 and that defect in exocytosis in *VAMP8* KO β cells is overcome by the increased β cell mass.

VAMP8 KO Amplifies GLP-1/Ex-4-Induced β Cell Proliferation

Increased β cell mass in *VAMP8* KO islets could be due to primary or secondary effects, including insulin secretory deficiency and peripheral insulin resistance leading to compensatory β cell proliferation (Kahn, 1998). The latter seems unlikely since *VAMP8* KO mice assessed by insulin tolerance test were not insulin resistant (Figure 4C). In Figure 4D, we have shown that plasma incretin levels that could affect islet mass were not altered.

We thus postulated that VAMP8 affects β cell proliferation by a mechanism distinct from its actions on the exocytotic machinery. We examined factors in *VAMP8* KO islets that could account for β cell proliferation, including Pdx1, a critical transcription factor for β cell proliferation and survival (WT, 100%; *VAMP8* KO, 172% \pm 19.4%), and cell-cycle protein cyclin D1, a mediator for β cell proliferation (WT, 100%; *VAMP8* KO, 150.3% \pm 10.5%), which were at higher levels in *VAMP8* KO than WT islets at basal conditions (Figure 5A). There has been much ado about GLP-1-based therapies that increase islet β cell mass in diabetes patients (Lovshin and Drucker, 2009). To assess whether *VAMP8* KO deletion might induce islet β cells to become more conducive to Ex-4-induced proliferation, we examined the *in vivo* effects of Ex-4 on β cell mass. *VAMP8* KO and WT mice were treated twice daily with Ex-4 injections for three consecutive days, and on the fourth day pancreata were isolated and subjected to several assays: islet isolation for western blot analysis, and pancreatic tissue sectioning for islet morphometry and histochemical analysis. Ex-4 treatment caused the already higher basal levels of cyclin D1 to increase by a 477% in *VAMP8* KO islets compared to a lower 226% increase in WT islets (Figure 5B). Pdx1 levels were mildly increased in *VAMP8* KO (from 152% to 264%) and WT islets (from 100% to 165%). Ex-4 treatment caused a stronger \sim 85% increase in β cell area in KO islets (Figure 5C; WT, 0.0052 \pm 0.0006; KO, 0.0096 \pm 0.0017; $p < 0.05$). With already higher basal levels of Ki67 in *VAMP8* KO islets (WT, 0.38% \pm 0.05%; KO, 0.88% \pm 0.16%; Figure 4F), Ex-4 caused a higher increase of 186% in Ki67 levels (Figure 5D, brown colored cells in Figure 5E) in *VAMP8* KO islets (2.52% \pm 0.55%; $p < 0.05$) versus 145% increase in WT islets (WT, 0.93 \pm 0.13%, $p < 0.05$). To assess whether Ex-4 treatment *per se* caused these increases beyond those attributed to the *VAMP8* genotype, we analyzed the data as the ratio of KO/WT and fold increase (Table S1), which showed that Ex-4 *per se* increased more so in *VAMP8* KO than in WT islet β cell area, Ki67, and cyclin D1 levels but not Pdx1.

Polo-like kinase 1 (Plk1), an activator of several stages in mitosis, particularly centriole activity (Tsou et al., 2009), was more abundant in islets within *VAMP8* KO mouse pancreas sections (Figure 5F), which was confirmed at protein level by isolation of the islets after *in vivo* Ex-4 treatment. Here, basal islet levels of Plk1 (Figure 5G) were already higher in *VAMP8* KO islets

(KO, 269%; WT, designated as 100%). Ex-4 treatment caused a 229.8% increase in islet Plk1 protein levels in *VAMP8* KO islets (886.4% of WT basal levels) compared to very little increase of 21.7% in WT islets (121.7%). Apoptotic processes seemed unaltered by *VAMP8* deletion as islet levels of total caspase 3 and cleaved (activated) caspase 3 were not different between *VAMP8* KO and WT islets (data not shown).

Because of the possibility of unforeseen confounding *in vivo* factors that can account for β cell proliferation, mouse islets were isolated and treated *ex vivo* with Ex-4 for 48 hr and dispersed into single β cells for imaging analysis of Plk1 and BrdU incorporation. Ex-4 caused basal Plk1 activity (Figure 5H) in *VAMP8* KO β cells (4.26 \pm 0.57, similar to 3.5 \pm 0.26 in WT β cells) to increase by 239% (14.43 \pm 0.63) which was higher ($p = 0.03$) than the 134% increase in WT β cells (8.27 \pm 0.85). BrdU incorporation (indicator of active DNA replication, Figure 5I), although similar between *VAMP8* KO and WT β cells at basal condition (12.02 \pm 0.85 versus 6.73 \pm 2.79 in WT β cells, $p = 0.07$), Ex-4 caused a much larger increase of 307% in *VAMP8* KO β cells (48.88 \pm 2.62, $p = 0.02$) compared to 181% increase in WT β cells (18.94 \pm 3.44).

These results taken together indicate that *VAMP8* deletion *per se* was the primary driver of increased β cell growth, which was amplified further by GLP1/Ex-4 treatment.

VAMP8 Depletion Enhances β Cell Mitosis

VAMP8 actions on β cell proliferation are likely mediated by mechanisms distinct from that directly affecting insulin exocytosis. In fact, several reports showed that VAMP8 is localized to the midbody during midbody abscission in cell division to daughter cells, whereby dominant-negative VAMP8 (Low et al., 2003) or siRNA downregulation of VAMP8 expression (Schiel et al., 2011) blocked midbody abscission. These studies were nonetheless performed on cell lines (MDCK, HeLa cells). It was thus opportune to examine the possible role of VAMP8 in islet β cell mitosis, employing *VAMP8* KO islet β cells (Figures 6D and 6E) and siRNA downregulation of VAMP8 expression in INS-1 cells (Figures 6B and 6C) in response to Ex-4-induced proliferation. We assessed the distribution of α -tubulin (green) as a marker for microtubules (Figure 6), which exhibit different patterns of web-like cytosolic distribution during the stages of mitosis (Figures 6A, 6B, and 6D approximate the mitotic stages depicted in the cartoons). In 10 nM Ex- (16–24 hr) treated control INS-1 cells (Figure 6A), as expected (Low et al., 2003; Schiel et al., 2011), VAMP8 (red) accumulated at sites of microtubule concentration (yellow, merge images) within mitotic structures (top to bottom: metaphase, anaphase, telophase). In telophase, microtubules appear to concentrate at intercellular bridges of narrowing cleavage furrows between dividing daughter cells (Figure 6B, third image; Figure 6C, bottom); this is precisely where VAMP8 is located in control cells (Figure 6A, bottom). Remarkably, VAMP8 siRNA-treated INS-1 cells (88.2% knock-down, Figures 6B and 6C) showed a higher percentage (4.6-fold) of mitosis (5.48% \pm 0.73%) compared to scrambled siRNA-treated INS-1 cells (1.20% \pm 0.51%). Whereas WT islet β cells have low capacity to undergo mitosis, 48 hr Ex-4 (10 nM) treatment of isolated *VAMP8* KO (Figure 6D) islets (then dispersed into single β cells) caused a much higher percentage (3.3-fold) of mitosis (0.50% \pm 0.13%) than WT β cells

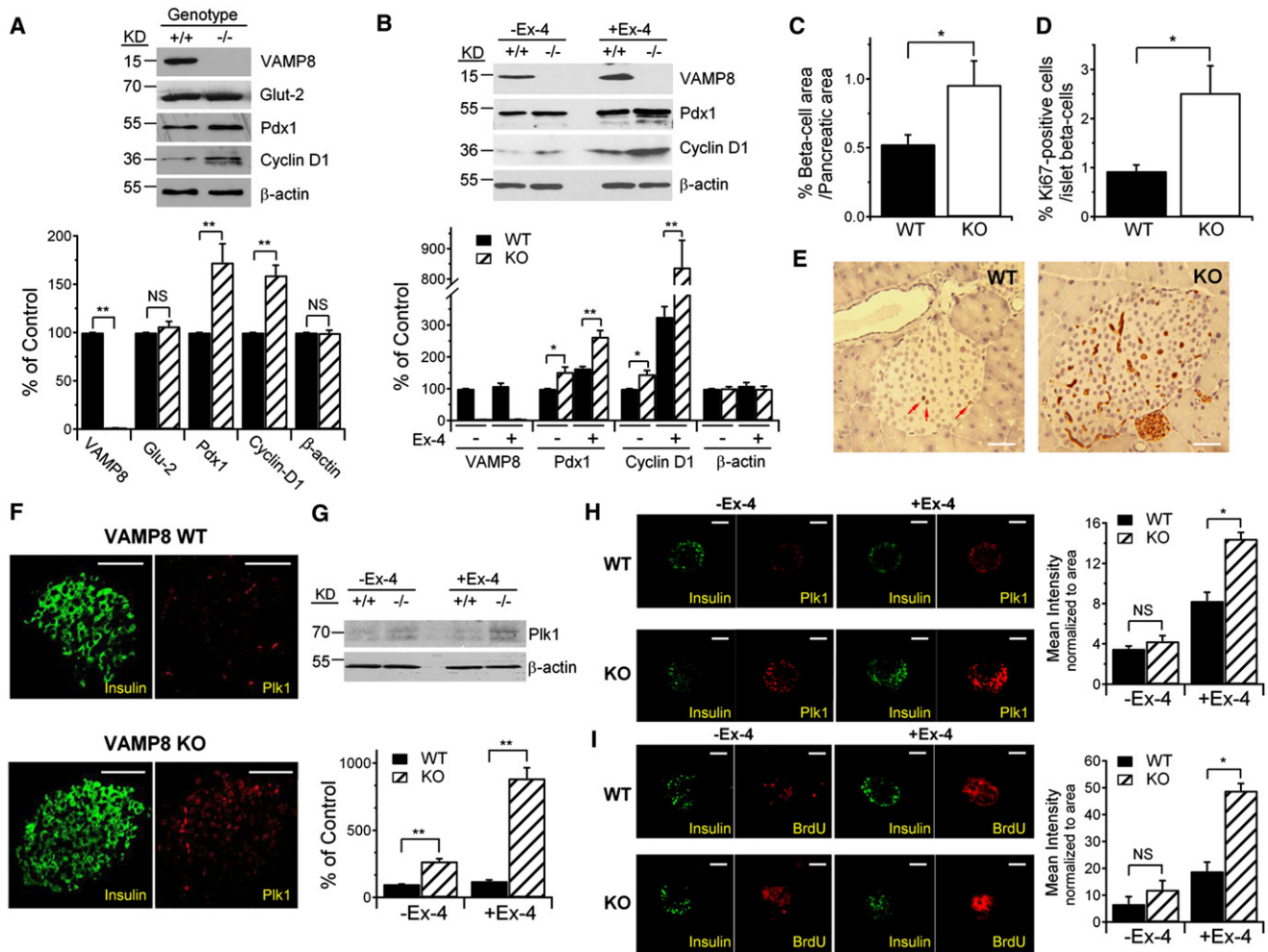


Figure 5. VAMP8 Deletion Amplifies GLP-1/Ex-4-Induced β Cell Proliferation

(A and B) Western blots identifying the indicated proteins in WT (+/+) and *VAMP8* KO (−/−) mouse islets. In (A), n = 4. Separate experiments were done in absence and presence of in vivo Ex-4 treatment. In (B), n = 4, with the respective densitometry analyses shown in the corresponding bottom panels. Values from WT islets without Ex-4 treatment were used as a control (100%), wherein all other values were normalized to the control.

(C) β cell area per pancreatic area was calculated on insulin-stained pancreatic sections in in vivo Ex-4-treated WT and *VAMP8* KO mice. n = 10 mice each.

(D) Ki67-positive islet β cell, as percentage of total islet β cells, in in vivo Ex-4-treated WT and *VAMP8* KO mice. n = 10 mice each.

(B–D) Additional analyses of the data in (B) (Cyclin D1, Pdx-1), (C) (β cell area), and (D) (Ki67) are in Table S1 to assess whether increases in these factors are due to *VAMP8* KO genotype or Ex-4 induction per se.

(E) Islet architecture shown by Ki67 staining on pancreatic sections (red arrows indicate Ki67-positive signals in WT; red signals indicate Ki67-positive signals in KO). Scale bars represent 20 μ m.

(F and G) *VAMP8* KO pancreatic β cell exhibit increased mitotic activity.

(F) Representative immunofluorescence images of islet insulin (green) and Plk1 (red) in pancreas sections of in vivo Ex-4-treated mice. Scale bars represent 50 μ m.

(G) Western blot showing islet levels of polo-kinase 1 (Plk1) (top panel) and blot analysis (bottom panel) of four experiments.

(H and I) Representative immunofluorescence images (left panels) and summary graphs of the staining intensity (right panels) from littermate WT and *VAMP8* KO islet β cells stained for insulin (green), Plk1 (red) (H), or with BrdU incorporation (red) (I). Here, isolated islets were treated ex vivo with or without Ex-4 as indicated. Scale bars represent 5 μ m. n = 10–15 cells per group.

Summary graphs are shown as means \pm SEMs. *p < 0.05, **p < 0.01; NS, not significant.

See also Table S1.

(0.15% \pm 0.06%) (Figure 6E). These results indicate that *VAMP8* deletion per se increases Ex-4 induction of β cell mitosis.

DISCUSSION

In this work, we have identified a dual role for *VAMP8* in islet β cells. First is *VAMP8*'s role in insulin SG exocytosis, which is

by mechanisms distinct from its second role in β cell proliferation, the latter at least in part by *VAMP8*'s actions on mitosis. Below we discuss these two major findings.

Our first major finding is that *VAMP8* mediates recruitment of newcomer insulin SGs to the PM, contributing to biphasic GSI. In spite of possessing the major exocytotic machinery of neurons (Syn-1/Munc18a), β cell is a rather slow secretory

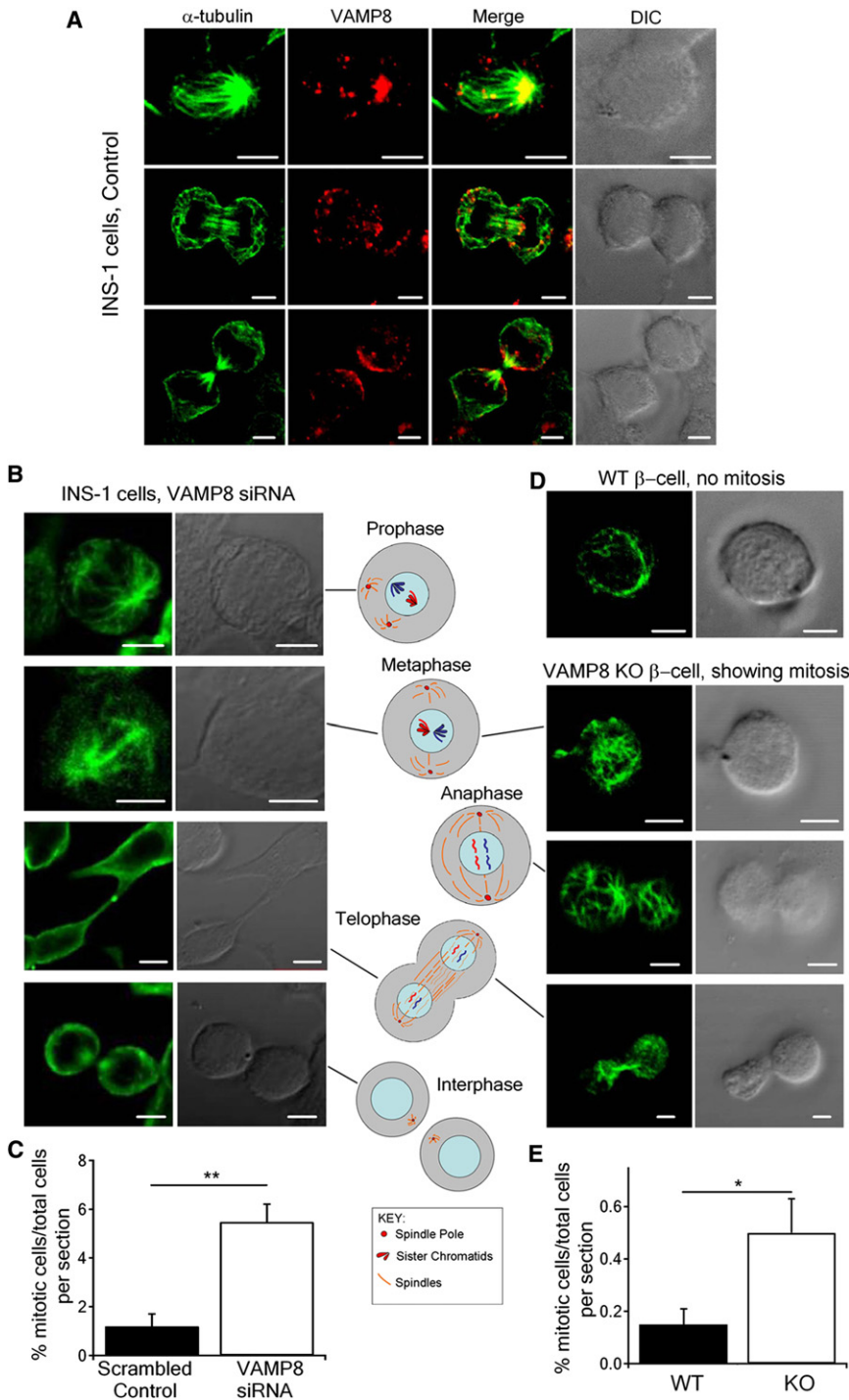


Figure 6. VAMP8 Deletion Enhances Ex-Induced β Cell Mitosis

(A) In INS-1 cells treated with 10 nM Ex-4, VAMP8 (red) accumulates in regions of α -tubulin (green) concentration, the latter to identify the changes in pattern of microtubules in different stages of mitosis. Shown are representative images of four independent experiments.

(B and C) INS-1 cells transduced with VAMP8 siRNA then treated with Ex-4 (10 nM, 16–24 hr) caused a greater increase in mitosis compared to scrambled siRNA Control.

(D and E) Single islet β cells treated with 10 nM Ex-4 (48 hr) from VAMP8 KO mice (bottom, showing various stages of mitosis) exhibited much higher rate of mitosis than β cells of WT mice (top, showing no mitosis).

Quantitative analysis (means \pm SEMs) of percentage of mitotic structures in β cells per section is shown in (C) from three independent experiments ($n = 20$ sections per group) for (B), and (E) from three independent experiments ($n = 28$ sections per group) for (D). * $p < 0.05$, ** $p < 0.01$. Scale bars represent 5 μ m. Cartoons of stages of mitosis are shown, corresponding to mitotic structures shown in (B) and (D) as indicated.

Munc18a/Syn-1A assembly with VAMP2/SNAP25 (Ohara-Imaizumi et al., 2007) but also by a larger contribution from newcomer SGs (Seino et al., 2009). It thus seems that for exocytosis of insulin SGs in β cells, SG docking per se is not a prerequisite but rather a temporal constraint for fusion with the PM (Kasai et al., 2008). From these reports, two populations of newcomer SGs were identified, those that undergo rapid fusion with minimal or no docking time (we called “no-dock” SGs) and those exhibiting longer docking time (“short-dock” SGs). In first-phase GSIS, the population of short-dock SGs, whose exocytosis was not affected by VAMP8 deficiency, might share the same exocytotic machinery as predocked SGs employing neuronal Munc18a/Syn-1A/SNAP-25 complex with VAMP2. This suggests that newcomer SGs undergoing minimal docking time could be mediated by VAMP8 in complex with Syn-2, Syn-3, or both, along with SNAP25 and

cell with reduced capacity for primary exocytosis of docked SGs compared to neurons. β cells have ability to compensate for this inefficiency with two additional modes of exocytosis, including recruitment of newcomer SGs and to lesser degree, SG-SG fusion (Gaisano, 2012). Rapid recruitment of newcomer SGs has been described by several laboratories (Kasai et al., 2008; Shibasaki et al., 2007; Yasuda et al., 2010). In β cells, first-phase GSIS is contributed not only by docked SGs mediated by

Munc18b. Takahashi et al. (2010) elegantly demonstrated that in β cells, some regions on the PM have SNARE complexes (Syn-1A/SNAP25) preassembled enabling rapid exocytosis, while at other regions SNARE assembly was slower which could account for slower exocytosis. This suggests the possibility of more rapid assembly of VAMP8-SM/SNARE complexes to mediate rapid exocytosis of newcomer SGs. In support of this, VAMP8 depletion reduced the stability of Syn-2 and Syn-3

assembly with SNAP25 (and SNAP23). What are the potential facilitators of rapid SM/SNARE complex assembly? CDK5 phosphorylation of Munc18b was reported to induce Munc18b/SNARE complex (Syn-3/SNAP25/VAMP2) assembly (Liu et al., 2007). Kasai et al. (2008) suggested that Rab27a can hasten mobility and fusion of newcomer SGs. β cell GLP-1 receptor activation acts through cAMP/PKA signaling to accelerate recruitment and fusion of newcomer SGs. Although VAMP8, Syn-2, Syn-3, or SNAP25 do not possess consensus sites for cAMP or PKA phosphorylation (by Motif Scan search, http://scansite.mit.edu/motifscan_id.phtml), PKA phosphorylation of snapin might interact with these SM/SNARE complexes to augment insulin secretion (Song et al., 2011). Perhaps GLP-1-mediated activation of cAMP-GEF2 and PKA phosphorylation of RIM2, shown to accelerate recruitment of newcomer SGs (Seino et al., 2009; Shibasaki et al., 2007; Yasuda et al., 2010), may be interacting and perhaps even drive VAMP8 SM/SNARE fusion complex formation. This is likely, as our protocols included IBMX that raises cAMP levels and amplified GLP-1. Homotypic SG-SG fusion in β cells, in the form of sequential exocytosis, occurs infrequently and contributes relatively little to biphasic GSIS (Takahashi et al., 2002, 2004). Whether VAMP8 exocytotic complexes play a role in insulin SG-SG fusion requires further study with more-appropriate strategies, such as two-photon microscopy (Takahashi et al., 2002; 2004). We also do not know whether there are actually separate subpopulations of SGs possessing different VAMPs or a single SG population containing both VAMP2 and VAMP8 that compete for assembly with distinct activated Munc18/Syn complexes to mediate these distinct exocytotic events.

The second major finding in this work is that VAMP8 negatively regulates β cell proliferation, a major target that we postulated to be β cell mitosis. VAMP8 and cognate Syntaxin 2 were postulated to participate in the terminal step of cytokinesis (Low et al., 2003), which is abscission of midbody of two daughter cells undergoing cell division. That study employed overexpression of a dominant-negative nonmembrane-anchored VAMP8 mutant, which probably blocked other VAMPs. However, a more recent study showed that siRNA depletion of VAMP8 also blocked midbody abscission (Schiel et al., 2011) and that VAMP8 from recycling endosomes was recruited to fuse with the furrow membrane, particularly at telophase. Those reports have used cell lines (MDCK, HeLa cells). Consistently, VAMP8 is present in endosomes of islet β cells and is concentrated in microtubule regions of β cells where they can actively regulate mitotic cell division. However, in contrast to those reports, our study showed that VAMP8 deletion per se promoted β cell proliferation by specific actions on promoting β cell mitosis per se, including upregulation of mitotic factors cyclin D1 and Plk1, the latter affecting centriole activity during cell division. These events seemed to be cell context specific since embryonic fibroblasts and exocrine pancreas in VAMP8 KO mice exhibited normal cell division (Wang et al., 2004), indicating that its role in fibroblast and acini cytokinesis could be replaced by other VAMPs. Furthermore, VAMP8 deletion-induced increase in β cell proliferative activity seems to occur after birth. In β cells, we postulate that VAMP8's role might be that of an inhibitory v-SNARE (Varlamov et al., 2004) rather than a v-SNARE that promotes fusion of mitotic cleavage furrow in MDCK and HeLa

cell lines employed in previous studies. Alternatively, VAMP8 might act as a competing weaker partial agonist v-SNARE in β cells, wherein the absence of VAMP8 removes this negative regulation, allowing a more potent undefined v-SNARE to promote β cell mitosis. This would provide a fine-tuning for cytokinesis. GLP-1's ability to induce β cell proliferation was amplified by VAMP8 deficiency, suggesting that GLP-1 action might at least in part be inactivating VAMP8 during mitosis.

The precise mechanisms by which GLP-1 receptor signaling in islet β cells is coupled to its many actions, particularly insulin secretion and β cell growth, are not completely understood, and many gaps remain in spite of the very large amount of work and collective effort. We hope that our work has shed some additional insight. We showed here that GLP-1 potentiation of GSIS here was in part contributed to by VAMP8-mediated recruitment of newcomer SGs to the PM. To balance its secretory function, perhaps to avoid a hypersecretory state that would be deleterious for glucose homeostasis, VAMP8 may execute a negative block on β cell proliferation. These two VAMP8-mediated apparently opposing events affected by distinct mechanisms, may underlie some of the therapeutic actions of GLP-1 on insulin secretion and β cell growth. It will be interesting to examine whether levels or modification of VAMP8 interactions with cognate exocytotic proteins are regulated by physiological or pathological (T2DM) perturbation. It is envisioned that lower levels of VAMP8 may induce β cell proliferation, and higher levels may restrict β cells to a lower basal proliferative rate, conferring an important fine-tuning regulatory role for VAMP8 as an inhibitory SNARE (Varlamov et al., 2004) on β cell mitosis. The inherent secretory inefficiency of β cells is further accentuated in T2DM in part by reduction in islet levels of the synaptic exocytotic machinery (Munc18a/Syn-1A/SNAP25/VAMP2) (Ostenson et al., 2006) that mediates exocytosis of docked SGs. This β cell secretory inefficiency could be compensated by the VAMP8 exocytotic machinery, which recruits a large population of newcomer SGs exceeding the population of docked SGs. In sum, we have demonstrated a dual role of VAMP8 on exocytosis and mitosis in β cells.

EXPERIMENTAL PROCEDURES

Mouse Genetics and Islet Isolation

VAMP8 KO mice were generated and backcrossed seven generations in 129SvJ background as previously described (Wang et al., 2004, 2007). Genotyping was performed as reported (Wang et al., 2004). All analyses in this paper on constitutive KO mice were performed with age-matched littermate control (WT mice). Animal procedures were performed in accordance with the University of Toronto's Animal Care Committee's ethical guidelines. Islets were prepared as previously described (Kwan and Gaisano, 2005).

Western Blotting and Immunoprecipitation Assay

Western blots of islet lysate samples were performed with the indicated antibodies as detailed in the Supplemental Experimental Procedures. Immunoprecipitation assays using Syn-1, Syn-2, and Syn-3 antibodies were conducted on INS-1 cells as also described in detail in the Supplemental Experimental Procedures.

Islet Perfusion Assay

Batches of 50 mouse islets were stimulated with glucose in the presence or absence of 10 nM GLP-1 (7–36) amide plus 3-isobutyl-1-methylxanthine (IBMX; 150 μ M) as previously reported (Kwan et al., 2007), with secreted insulin

determined by RIA (Linco Research). Insulin secreted was normalized to total insulin content.

Confocal Immunofluorescence Microscopy

This was performed as described in the [Supplemental Experimental Procedures](#) with a laser-scanning confocal imaging system (LSM510, Carl Zeiss), and image analysis performed by NIS-Elements AR 3.0 (Nikon).

Electrophysiology

Cells were patch-clamped in conventional whole-cell configuration as described in the [Supplemental Experimental Procedures](#). Cm measurements performed with an EPC-9 amplifier and PULSE software (HEKA Elektronik) as described (Kwan et al., 2007) and data analyzed with Igor Pro software (WaveMetrics).

TIRF Imaging and Data Analysis

TIRFM images were acquired by a Nikon TE2000U TIRF microscope at 5 Hz with a 100 ms exposure time. Insulin SG mobilization and exocytosis were analyzed by Matlab (Math Works), ImageJ (NIH), and Igor Pro software. Further information about the TIRF microscopy configuration, TIRFM imaging, single-SG exocytosis, and analysis are detailed in the [Supplemental Experimental Procedures](#).

Exendin-4 Treatments, IPGTT, IPITT, and OGTT

Synthetic exendin-4 (Bachem) was administered to 6- to 8-week-old mice by i.p. injection twice daily for three consecutive days at a dose of 24 nmol/kg body weight. Age-matched PBS-injected mice were used as controls. Pancreases were excised and analyzed as described below. IPGTT, IPITT, and OGTT were performed as described in the [Supplemental Experimental Procedures](#).

Islet Morphometry, Immunohistochemistry, and Immunofluorescence Assay

Sections (7 μ m thick) were obtained as described previously (Choi et al., 2010), immunostained for insulin, Ki67 (DAKO), and glucagon (NovoCastra Laboratories). Total β cell area, islet number, and total pancreatic area were determined on insulin-stained sections. Total β cell area, total islet number, and Ki67 analysis were calculated per total pancreatic area. Immunofluorescence-stained sections were visualized with a Zeiss inverted fluorescence microscope.

Statistical Analysis

All data are presented as means \pm SEM. Statistical significance was assessed by repeated-measure ANOVA, or Student's t test in SigmaStat (Systat Software). Significant difference is indicated by asterisks (* p < 0.05, ** p < 0.01, *** p < 0.001).

SUPPLEMENTAL INFORMATION

Supplemental Information includes Supplemental Experimental Procedures, four figures, and one table and can be found with this article online at <http://dx.doi.org/10.1016/j.cmet.2012.07.001>.

ACKNOWLEDGMENTS

We thank L. Sheu, H. Xie, and G. Flock for technical assistance. This work was supported by grants to H.Y.G. (Canadian Institute of Health Research [CIHR] MOP 89889 and MOP 86544) and M.W. (CIHR MOP 201188). D.Z. and S.D. were funded by fellowships from the Banting and Best Diabetes Centre, University of Toronto. Graduate studentships were from the CIHR (to P.P.L.L. and D.C.) and Canadian Diabetes Association (to E.P.C. and D.C.).

Received: August 2, 2011

Revised: April 17, 2012

Accepted: June 26, 2012

Published online: July 26, 2012

REFERENCES

- Antonin, W., Holroyd, C., Fasshauer, D., Pabst, S., Von Mollard, G.F., and Jahn, R. (2000a). A SNARE complex mediating fusion of late endosomes defines conserved properties of SNARE structure and function. *EMBO J.* **19**, 6453–6464.
- Antonin, W., Holroyd, C., Tikkanen, R., Höning, S., and Jahn, R. (2000b). The R-SNARE endobrevin/VAMP-8 mediates homotypic fusion of early endosomes and late endosomes. *Mol. Biol. Cell* **11**, 3289–3298.
- Choi, D., Schroer, S.A., Lu, S.Y., Wang, L., Wu, X., Liu, Y., Zhang, Y., Gaisano, H.Y., Wagner, K.U., Wu, H., et al. (2010). Erythropoietin protects against diabetes through direct effects on pancreatic beta cells. *J. Exp. Med.* **207**, 2831–2842.
- Cosen-Binker, L.I., Binker, M.G., Wang, C.C., Hong, W., and Gaisano, H.Y. (2008). VAMP8 is the v-SNARE that mediates basolateral exocytosis in a mouse model of alcoholic pancreatitis. *J. Clin. Invest.* **118**, 2535–2551.
- Dor, Y., Brown, J., Martinez, O.I., and Melton, D.A. (2004). Adult pancreatic beta-cells are formed by self-duplication rather than stem-cell differentiation. *Nature* **429**, 41–46.
- Gaisano, H.Y. (2012). Deploying insulin granule-granule fusion to rescue deficient insulin secretion in diabetes. *Diabetologia* **55**, 877–880.
- Kahn, B.B. (1998). Type 2 diabetes: when insulin secretion fails to compensate for insulin resistance. *Cell* **92**, 593–596.
- Kasai, K., Fujita, T., Gomi, H., and Izumi, T. (2008). Docking is not a prerequisite but a temporal constraint for fusion of secretory granules. *Traffic* **9**, 1191–1203.
- Kwan, E.P., and Gaisano, H.Y. (2005). Glucagon-like peptide 1 regulates sequential and compound exocytosis in pancreatic islet beta-cells. *Diabetes* **54**, 2734–2743.
- Kwan, E.P., and Gaisano, H.Y. (2009). Rescuing the subprime meltdown in insulin exocytosis in diabetes. *Ann. N Y Acad. Sci.* **1152**, 154–164.
- Kwan, E.P., Xie, L., Sheu, L., Ohtsuka, T., and Gaisano, H.Y. (2007). Interaction between Munc13-1 and RIM is critical for glucagon-like peptide-1 mediated rescue of exocytotic defects in Munc13-1 deficient pancreatic beta-cells. *Diabetes* **56**, 2579–2588.
- Lippert, U., Ferrari, D.M., and Jahn, R. (2007). Endobrevin/VAMP8 mediates exocytotic release of hexosaminidase from rat basophilic leukaemia cells. *FEBS Lett.* **581**, 3479–3484.
- Liu, Y., Ding, X., Wang, D., Deng, H., Feng, M., Wang, M., Yu, X., Jiang, K., Ward, T., Aikhionbare, F., et al. (2007). A mechanism of Munc18b-syntaxin 3-SNAP25 complex assembly in regulated epithelial secretion. *FEBS Lett.* **581**, 4318–4324.
- Loo, L.S., Hwang, L.A., Ong, Y.M., Tay, H.S., Wang, C.C., and Hong, W. (2009). A role for endobrevin/VAMP8 in CTL lytic granule exocytosis. *Eur. J. Immunol.* **39**, 3520–3528.
- Lovshin, J.A., and Drucker, D.J. (2009). Incretin-based therapies for type 2 diabetes mellitus. *Nat Rev Endocrinol* **5**, 262–269.
- Low, S.H., Li, X., Miura, M., Kudo, N., Quiñones, B., and Weimbs, T. (2003). Syntaxin 2 and endobrevin are required for the terminal step of cytokinesis in mammalian cells. *Dev. Cell* **4**, 753–759.
- Ohara-Imaizumi, M., Fujiwara, T., Nakamichi, Y., Okamura, T., Akimoto, Y., Kawai, J., Matsushima, S., Kawakami, H., Watanabe, T., Akagawa, K., and Nagamatsu, S. (2007). Imaging analysis reveals mechanistic differences between first- and second-phase insulin exocytosis. *J. Cell Biol.* **177**, 695–705.
- Ostenson, C.G., Gaisano, H., Sheu, L., Tibell, A., and Bartfai, T. (2006). Impaired gene and protein expression of exocytotic soluble N-ethylmaleimide attachment protein receptor complex proteins in pancreatic islets of type 2 diabetic patients. *Diabetes* **55**, 435–440.
- Ren, Q., Barber, H.K., Crawford, G.L., Karim, Z.A., Zhao, C., Choi, W., Wang, C.C., Hong, W., and Whiteheart, S.W. (2007). Endobrevin/VAMP-8 is the primary v-SNARE for the platelet release reaction. *Mol. Biol. Cell* **18**, 24–33.
- Rorsman, P., and Renström, E. (2003). Insulin granule dynamics in pancreatic beta cells. *Diabetologia* **46**, 1029–1045.

- Sadoul, K., Berger, A., Niemann, H., Weller, U., Roche, P.A., Klip, A., Trimble, W.S., Regazzi, R., Catsicas, S., and Halban, P.A. (1997). SNAP-23 is not cleaved by botulinum neurotoxin E and can replace SNAP-25 in the process of insulin secretion. *J. Biol. Chem.* *272*, 33023–33027.
- Schiel, J.A., Park, K., Morphey, M.K., Reid, E., Hoenger, A., and Prekeris, R. (2011). Endocytic membrane fusion and buckling-induced microtubule severing mediate cell abscission. *J. Cell Sci.* *124*, 1411–1424.
- Seino, S., Takahashi, H., Fujimoto, W., and Shibasaki, T. (2009). Roles of cAMP signalling in insulin granule exocytosis. *Diabetes Obes. Metab.* *11 (Suppl 4)*, 180–188.
- Shibasaki, T., Takahashi, H., Miki, T., Sunaga, Y., Matsumura, K., Yamanaka, M., Zhang, C., Tamamoto, A., Satoh, T., Miyazaki, J., and Seino, S. (2007). Essential role of Epac2/Rap1 signaling in regulation of insulin granule dynamics by cAMP. *Proc. Natl. Acad. Sci. USA* *104*, 19333–19338.
- Song, W.J., Seshadri, M., Ashraf, U., Mdluli, T., Mondal, P., Keil, M., Azevedo, M., Kirschner, L.S., Stratakis, C.A., and Hussain, M.A. (2011). Snapin mediates incretin action and augments glucose-dependent insulin secretion. *Cell Metab.* *13*, 308–319.
- Südhof, T.C., and Rothman, J.E. (2009). Membrane fusion: grappling with SNARE and SM proteins. *Science* *323*, 474–477.
- Takahashi, N., Kishimoto, T., Nemoto, T., Kadowaki, T., and Kasai, H. (2002). Fusion pore dynamics and insulin granule exocytosis in the pancreatic islet. *Science* *297*, 1349–1352.
- Takahashi, N., Hatakeyama, H., Okado, H., Miwa, A., Kishimoto, T., Kojima, T., Abe, T., and Kasai, H. (2004). Sequential exocytosis of insulin granules is associated with redistribution of SNAP25. *J. Cell Biol.* *165*, 255–262.
- Takahashi, N., Hatakeyama, H., Okado, H., Noguchi, J., Ohno, M., and Kasai, H. (2010). SNARE conformational changes that prepare vesicles for exocytosis. *Cell Metab.* *12*, 19–29.
- Tiwari, N., Wang, C.C., Brochetta, C., Ke, G., Vita, F., Qi, Z., Rivera, J., Soranzo, M.R., Zabucchi, G., Hong, W., and Blank, U. (2008). VAMP-8 segregates mast cell-preformed mediator exocytosis from cytokine trafficking pathways. *Blood* *111*, 3665–3674.
- Tsou, M.F., Wang, W.J., George, K.A., Uryu, K., Stearns, T., and Jallepalli, P.V. (2009). Polo kinase and separase regulate the mitotic licensing of centriole duplication in human cells. *Dev. Cell* *17*, 344–354.
- Varlamov, O., Volchuk, A., Rahimian, V., Doege, C.A., Paumet, F., Eng, W.S., Arango, N., Parlati, F., Ravazzola, M., Orci, L., et al. (2004). i-SNAREs: inhibitory SNAREs that fine-tune the specificity of membrane fusion. *J. Cell Biol.* *164*, 79–88.
- Wang, C.C., Ng, C.P., Lu, L., Atlashkin, V., Zhang, W., Seet, L.F., and Hong, W. (2004). A role for VAMP8/endobrevin in regulated exocytosis of pancreatic acinar cells. *Dev. Cell* *7*, 359–371.
- Wang, C.C., Shi, H., Guo, K., Ng, C.P., Li, J., Gan, B.Q., Chien Liew, H., Leinonen, J., Rajaniemi, H., Zhou, Z.H., et al. (2007). VAMP8/endobrevin as a general vesicular SNARE for regulated exocytosis of the exocrine system. *Mol. Biol. Cell* *18*, 1056–1063.
- Wang, C.C., Ng, C.P., Shi, H., Liew, H.C., Guo, K., Zeng, Q., and Hong, W. (2010). A role for VAMP8/endobrevin in surface deployment of the water channel aquaporin 2. *Mol. Cell Biol.* *30*, 333–343.
- Williams, D., and Pessin, J.E. (2008). Mapping of R-SNARE function at distinct intracellular GLUT4 trafficking steps in adipocytes. *J. Cell Biol.* *180*, 375–387.
- Wong, S.H., Zhang, T., Xu, Y., Subramaniam, V.N., Griffiths, G., and Hong, W. (1998). Endobrevin, a novel synaptobrevin/VAMP-like protein preferentially associated with the early endosome. *Mol. Biol. Cell* *9*, 1549–1563.
- Yasuda, T., Shibasaki, T., Minami, K., Takahashi, H., Mizoguchi, A., Uriu, Y., Numata, T., Mori, Y., Miyazaki, J., Miki, T., and Seino, S. (2010). Rim2alpha determines docking and priming states in insulin granule exocytosis. *Cell Metab.* *12*, 117–129.
- Zhao, P., Yang, L., Lopez, J.A., Fan, J., Burchfield, J.G., Bai, L., Hong, W., Xu, T., and James, D.E. (2009). Variations in the requirement for v-SNAREs in GLUT4 trafficking in adipocytes. *J. Cell Sci.* *122*, 3472–3480.
- Zong, H., Wang, C.C., Vaitheesvaran, B., Kurland, I.J., Hong, W., and Pessin, J.E. (2011). Enhanced energy expenditure, glucose utilization, and insulin sensitivity in VAMP8 null mice. *Diabetes* *60*, 30–38.